Nuclear Inst. and Methods in Physics Research B 444 (2019) 6–9

Contents lists available at ScienceDirect

Nuclear Inst. and Methods in Physics Research B

journal homepage: www.elsevier.com/locate/nimb

# Raman spectroscopy of $Ar^+$-irradiated graphite surfaces supporting platinum nanoparticles

Tetsuya Kimata[a,b,*,1], Kenta Kakitani[c,d], Shunya Yamamoto[d], Tetsuya Yamaki[d], Takayuki Terai[c,e], Kazutaka G. Nakamura[a,b,*]

[a] Laboratory for Materials and Structures, Tokyo Institute of Technology, 4259 Nagatsuta, Yokohama 226-8503, Japan
[b] Department of Materials Science and Engineering, Tokyo Institute of Technology, 4259 Nagatsuta, Yokohama 226-8503, Japan
[c] Department of Nuclear Engineering and Management, The University of Tokyo, 7-3-1 Hongo, Tokyo 113-8656, Japan
[d] Takasaki Advanced Radiation Research Institute, National Institutes for Quantum and Radiological Science and Technology, 1233 Watanuki, Takasaki 370-1292, Japan
[e] The Institute of Engineering Innovation, The University of Tokyo, 2-11-16 Yayoi, Tokyo 113-8656, Japan

ARTICLE INFO

*Keywords:*
Raman spectroscopy
Graphite
Ar-ion-irradiation
Pt nanoparticles
Rf magnetron sputtering

ABSTRACT

Ion irradiation is well-known as a versatile tool for manipulating the physical, chemical and magnetic properties of carbon materials. Recently, the ion-beam-induced defects in carbon supports for platinum (Pt) nanoparticles have been found to enhance catalytic activity during the oxygen reduction reaction. This finding suggests that the electronic structure of the Pt nanoparticles would be affected by the ion-beam-irradiated carbon support. Raman spectroscopy was performed on the highly oriented pyrolytic graphite (HOPG) following the irradiated with 380 keV argon ions ($Ar^+$) and the deposition of Pt nanoparticles using radio frequency (rf) magnetron sputtering. In this paper, we obtained the phonon correlation length from Raman spectrum, and estimated that approximately three point defects were present at the interface between each 5 nm Pt nanoparticle and the HOPG irradiated with $Ar^+$ at the fluence of $1.0 \times 10^{13}$ ions/cm$^2$.

## 1. Introduction

Ion irradiation introduces lattice defect and radiation damage which affect various physical, chemical and magnetic properties of the host materials [1]. The ion irradiation in graphite has been extensively studied in connection with the research such as ion implantation and graphite intercalation compounds, the graphite surface has been modified by particles irradiation using various ion species and kinetic energy [2–5].

We recently found that the oxygen reduction reaction activity of the Pt nanoparticles on an argon ion ($Ar^+$)-irradiated glassy carbon (GC) substrate was approximately twice that of nanoparticles on a non-irradiated GC substrate [6,7]. However, the mechanism responsible for the observed activity enhancement has not been revealed. In order to elucidate this mechanism by theoretical calculation such as DFT simulation, it is necessary to investigate the surface structure of the carbon support irradiated with $Ar^+$, in other words, the number of defects interacting with Pt nanoparticle. Although the studies of Raman spectroscopy for the defective graphite/graphene or the carbon nanocubes supporting Pt nanoparticles were reported previously [8–11], the ion-beam-irradiated graphite supporting Pt nanoparticles have not been investigated by Raman spectroscopy.

Pt nanoparticles deposited on a highly oriented pyrolytic graphite (HOPG) surface have been used as a model catalyst [12,13], e.g. a study on the influence of nitrogen-doped carbon support on catalytic activity of Pt nanoparticles [14]. In the work reported herein, we deposited Pt nanoparticles on both $Ar^+$-irradiated and pristine HOPG, using radio frequency (rf) magnetron sputtering, and then investigated the influence of the ion-beam irradiation and Pt deposition on the surface structure of carbon supports by Raman spectroscopy.

## 2. Experimental

An HOPG (Grade SPI-II, SPI Supplies, West Chester, PA) with dimensions of $10 \times 10 \times 1$ mm$^3$ was used in this study. Clean thin specimens were obtained from this bulk material using adhesive tape. $Ar^+$-irradiation was performed at an energy of 380 keV and fluences between $1.0 \times 10^{12}$ and $1.0 \times 10^{14}$ ions/cm$^2$, using the ion implanter at the Takasaki Ion Accelerators for Advanced Radiation Application (TIARA) facility at the Takasaki Advanced Radiation Research Institute,

* Corresponding authors at: Laboratory for Materials and Structures, Tokyo Institute of Technology, 4259 Nagatsuta, Yokohama 226-8503, Japan.
*E-mail addresses:* kimata.t.aa@m.titech.ac.jp (T. Kimata), nakamura.k.ai@m.titech.ac.jp (K.G. Nakamura).
[1] Also at Ground Systems Research Center, Ministry of Defense (ATLA), 2-9-54 Fuchinobe, Sagamihara 252-0206, Japan.

https://doi.org/10.1016/j.nimb.2019.02.005
Received 25 September 2018; Received in revised form 29 January 2019; Accepted 2 February 2019
0168-583X/ © 2019 Published by Elsevier B.V.

QST, Japan. These fluence values were estimated by taking the product of the ion beam current density (10 nA/cm$^2$) and the irradiation time. Pt nanoparticles were subsequently deposited on the HOPG surfaces by an rf magnetron sputtering method in a sample preparation chamber (base pressure $< 6 \times 10^{-5}$ Pa), using Ar as the sputtering gas at a pressure of 0.18 Pa. The plasma output, frequency and sputtering time were 20 W, 13.56 MHz and 60 s, respectively. Although the GC was used as a carbon support, the size and areal density of the deposited Pt nanoparticles obtained under the same condition were already investigated in previous studies [6,15]. The resulting Pt particle size was observed to be around 3–5 nm by transmission electron microscopy (TEM).

Raman spectroscopic analysis of the pristine and pre-irradiated HOPG surfaces before and after the Pt deposition was performed using a LabRAM HR Evolution Raman spectrometer (HORIBA, Ltd., Japan) over the wavenumber range of 500–2000 cm$^{-1}$ at a resolution of 1.60 cm$^{-1}$. Incident radiation at 532 nm was provided using a single mode green laser (Showa Optronics JUNO J050GS-16, Japan), at a power level below 5 mW, applied to a sample area with a diameter of approximately 15 μm. Raman spectra were obtained with a back-scattering configuration by accumulating the signal during a 5 min exposure, and analyzed by fitting all peaks to a Lorentzian profile after subtracting constant background.

## 3. Results and discussion

Fig. 1 shows the defect density depth profile calculated using the Monte Carlo method with the TRIM code [16] for 380 keV $Ar^+$ in graphite with an irradiation angle normal to the c-face. A graphite density of 2.2 g/cm$^3$ was applied during these calculations. The defect density was determined to be approximately 0.2 atoms/Å/ion at 10 nm and this value gradually increased to a depth of 250 nm. The TRIM code was unable to calculate the defect density at the surface (that is, at 0 nm).

The optical absorption coefficient of graphite at 532 nm was calculated to be 0.032 nm$^{-1}$ based on the equation $\alpha = 4 \times \pi \times k/532$ (where k = 1.3 is the extinction coefficient of graphite [17]). Therefore, Raman scattering by the sample was affected by both the surface and the interior of the sample. Variations in sensitivity with depth in the back-scattering configuration were evaluated using the normalized optical penetration factor $\exp(-\alpha x)$ (where $x$ is the depth from the upper surface), as shown in Fig. 1. The sensitivity varies in this manner because both the excitation and scattered light are absorbed by the sample. The depth to which the sample could be probed by Raman spectroscopy was estimated to be $1/2\alpha$, which in this case was 16 nm.

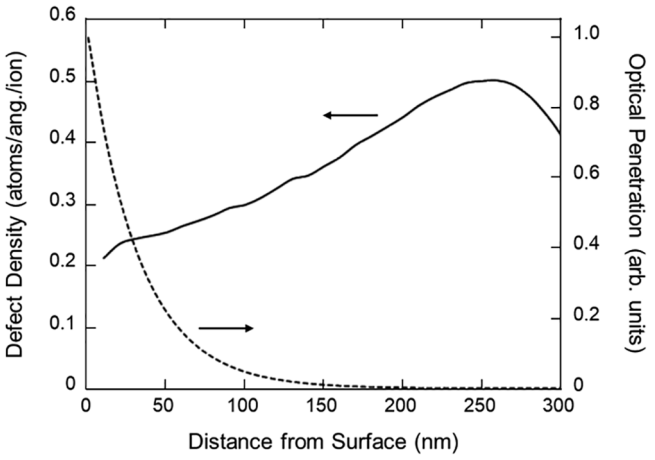


**Fig. 1.** The defect distribution depth profile following 380 keV $Ar^+$ irradiation of graphite as determined by TRIM calculations. The broken line represents the normalized optical penetration factor $\exp(-\alpha x)$ for 532 nm light in graphite.

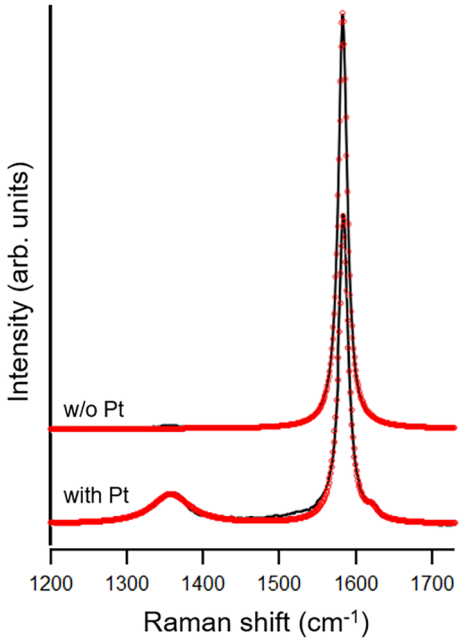


**Fig. 2.** The Raman spectra of the non-irradiated HOPG without (w/o) and with Pt deposition. Red circles and black curves represent experimental data and Lorentz curve fitting, respectively.

Fig. 2 presents the Raman spectra of the pristine HOPG and the HOPG supporting Pt nanoparticles. The spectrum of the pristine HOPG shows a sharp peak at 1583.5 cm$^{-1}$ with a full width at half maximum (FWHM) of approximately 13.7 cm$^{-1}$, attributed to the G peak of the graphite due to the in-plane $E_{2g}$ mode. In contrast, the spectrum from the HOPG with Pt nanoparticles exhibits two other peaks at 1356.9 and 1621.5 cm$^{-1}$ in addition to a slightly broadened G peak. These are known as the disorder induced peaks, and correspond to the D and D' peaks expected at approximately 1358 and 1615 cm$^{-1}$ [18]. The in-plane microcrystalline size ($L_a$) is typically determined from the peak intensity ratio ($R = I_D/I_G$), such that $L_a = 4.4/R$ (nm), where $I_G$ and $I_D$ represent the intensities of the G and D peaks [19,20], and previous studies have suggested that $L_a$ corresponds to the phonon correlation length [18,21]. This peak intensity was the area intensity acquired by Lorentzian fitting. The $L_a$ value for the HOPG with Pt nanoparticles was estimated to be 11.2 nm. This result that appearance of D peak in Raman spectrum of HOPG with Pt nanoparticles, and the lack of a D peak in the spectrum of the pristine HOPG, suggested that the HOPG surface had been damaged by the Pt deposition.

Raman spectra were also acquired from HOPG following irradiation with 380 keV $Ar^+$ and the deposition of Pt nanoparticles using the rf magnetron sputtering technique. Fig. 3 shows the spectra of the HOPG irradiated with $Ar^+$ at the fluences between $1.0 \times 10^{12}$ and $1.0 \times 10^{14}$ ions/cm$^2$ as obtained before and after Pt deposition. The Raman spectra of the samples excluding $1.0 \times 10^{14}$ ions/cm$^2$ were fitted by 3 peaks (G, D and D′ peaks), but that of the $1.0 \times 10^{14}$ ions/cm$^2$ sample were fitted by G and D peaks because a D′ peak was unremarkable in the spectra. The peak parameters obtained by curve fitting, including position and FWHM of G peak without and with Pt deposition are summarized in Fig. 4.

Fig. 4(a) shows the G peak position plotted against $Ar^+$ fluence. The significant peak-shift by the $Ar^+$-irradiation and Pt deposition was not observed on the fluence of under $1.0 \times 10^{13}$ ions/cm$^2$. On the fluence of over $5.0 \times 10^{13}$ ions/cm$^2$, the blueshift of the G peaks by the $Ar^+$-irradiation and the redshift of the G peaks by the Pt deposition were observed. The blueshift of the G bands by the $Ar^+$-irradiation was considered to correspond with the process from graphite to nanocrystalline graphite [22]. The higher the disorder in the structure, the lower

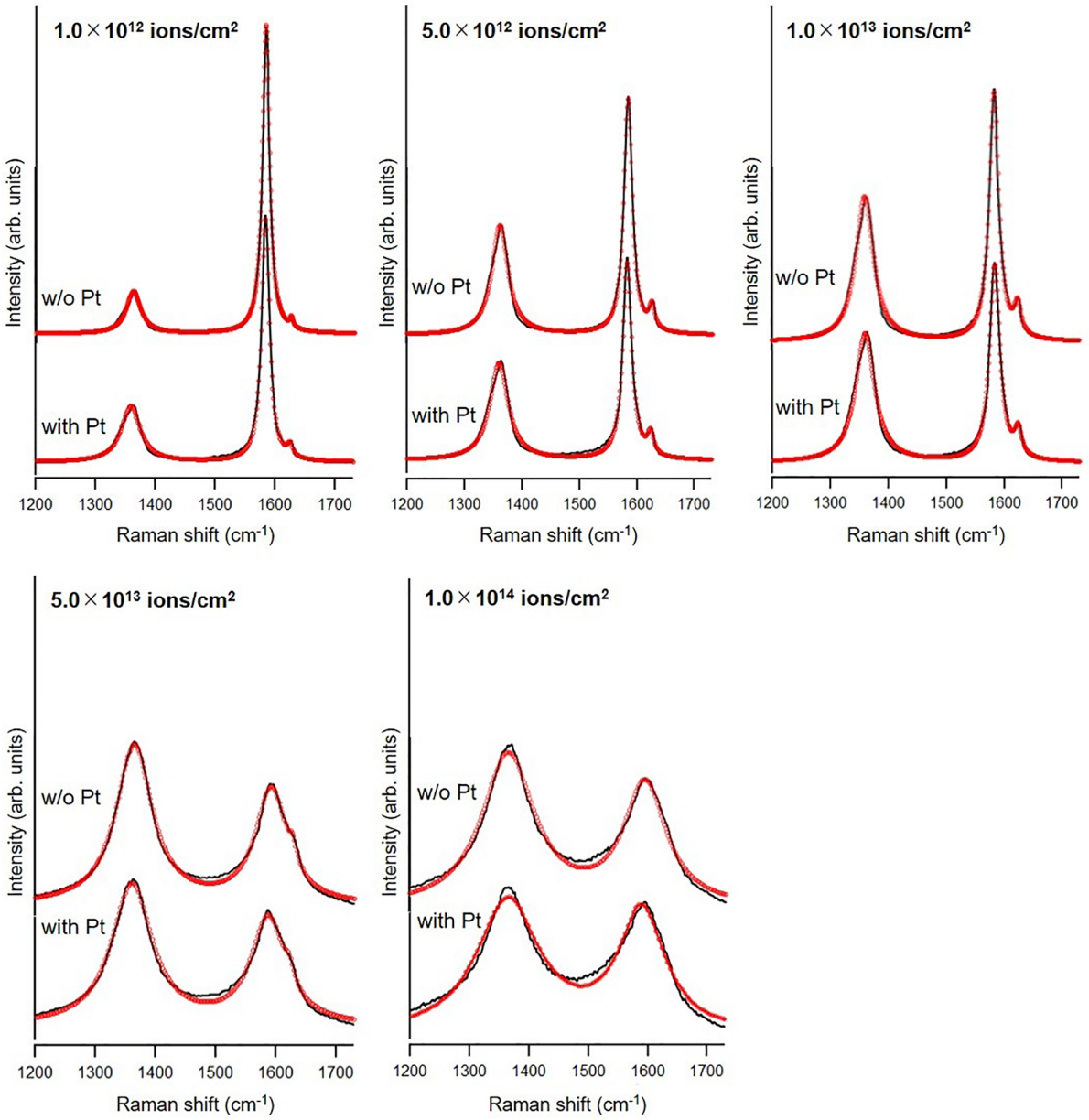


**Fig. 3.** The Raman spectra of the HOPG irradiated with $Ar^+$ at a fluence between $1.0 \times 10^{12}$ and $1.0 \times 10^{14}$ ions/cm$^2$ without and with Pt deposition. Red circles and black curves represent experimental data and Lorentz curve fitting, respectively.

the Raman shift of the G band and the larger its bandwidth [23,24], as can be seen from Fig. 4(b). This trend of the Raman shift was consistent with the redshift of the G peaks by the Pt deposition, and the trend of the bandwidth was also consistent with that of FWHM. The red shifts usually related to tensile stress caused by different lattice parameters of Pt and HOPG at various states of its ion beam modification. Interestingly, the red shift after Pt deposition becomes more obvious with higher degree of HOPG modification, i.e. after exposure to higher ion fluence. Electronic effects of Pt may contribute the redshift, because the electronic effect of Fe is reported on the redshifts in Raman scattering spectra of Fe-doped multi walled carbon nanotubes [25].

Fig. 5(a and b) shows the value of the R and $L_a$. The R is a measure of the disorder caused by the lattice damage; the value increased at higher fluence, and was further increased by Pt deposition except for the sample of $5.0 \times 10^{13}$ ions/cm$^2$. The increasing R directly denotes defectivity of the surface and sub-surface region. Pt deposition had lower effect on defectivity of the HOPG surface with increasing $Ar^+$-irradiation on the substrate prior deposition of Pt. The same principle applies for $L_a$ (Fig. 5(b)), the Pt deposition had lower effect on $L_a$ at higher fluence.

We calculated the mean distance ($L$) between in-plane defects using the defect density data in Fig. 1 (0.2 atoms/ang./ion at a depth of 10 nm) based on the equation $L = 1/\sqrt{(f \times N_d)}$, where $N_d$ is the number of defects and $f$ is the distance between the graphite layers (3.35 Å) [26,27]. The value of $N_d$ was estimated from the defect density and the fluence, and the $L$ value obtained when employing a fluence of $1.0 \times 10^{13}$ ions/cm$^2$ was 3.86 nm. This $L$ value calculated using the Fig. 1 data generated by the TRIM code is slightly shorter than the $L_a$ value estimated from the Raman spectrum (4.04 nm). This result suggested that the graphitic structure at a depth of 10 nm was more defective than at surface. We additionally investigated the number of lattice defects under the Pt nanoparticles for modeling of the interface structure between $Ar^+$-irradiated HOPG surface and Pt nanoprticles on the theoretical calculation. The $L_a$ value of the sample treated with a fluence of $1.0 \times 10^{13}$ ions/cm$^2$ and Pt deposition (3.59 nm) suggested that approximately three point defects were present at the interface

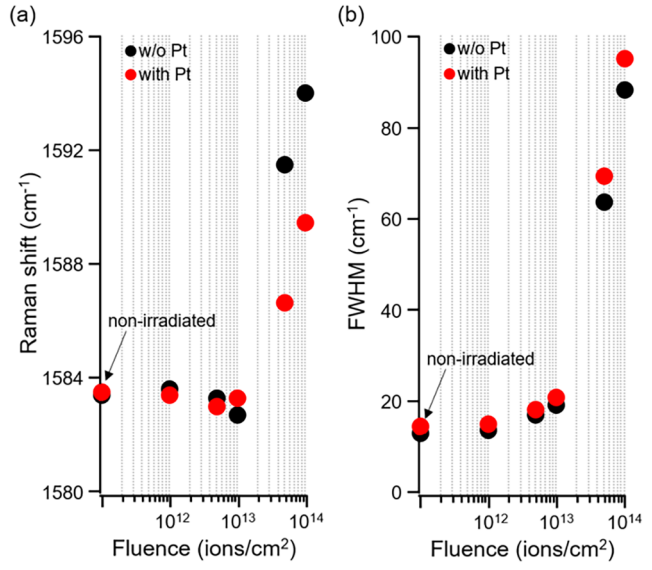


**Fig. 4.** The (a) position and (b) FWHM of the G peak plotted against $Ar^+$ fluence (black point: without Pt, red point: with Pt). (For interpretation of the references to colour in this figure legend, the reader is referred to the web version of this article.)

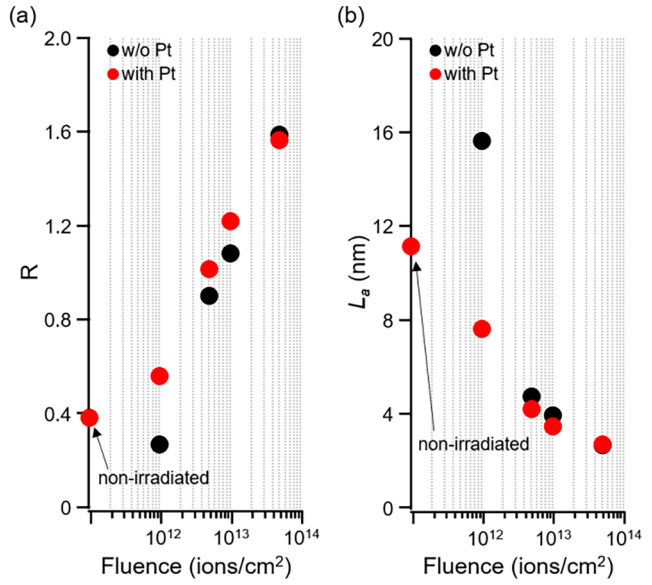


**Fig. 5.** The value of (a) R and (b) $L_a$ (black point: without Pt, red point: with Pt). (For interpretation of the references to colour in this figure legend, the reader is referred to the web version of this article.)

between each 5 nm Pt nanoparticle and the $Ar^+$-irradiated HOPG.

## 4. Conclusion

We employed Raman spectroscopy to study non-irradiated and $Ar^+$-irradiated HOPG before and after Pt deposition. The effect of Pt deposition induced damage was observed in Raman spectrum of the non-irradiated HOPG, and also observed slightly in that of the $Ar^+$-irradiated HOPG. Pt deposition showed more significant red Raman shift of G peak with increasing $Ar^+$ fluence, whereas it interestingly had an opposite effect on $L_a$. We also estimated that approximately three point defects were present at the interface structure between each 5 nm Pt nanoparticle and the HOPG irradiated with $Ar^+$ at the fluence of $1.0 \times 10^{13}$ ions/cm$^2$.

## Acknowledgments

We would like to thank C. Suzuki for her experimental support of TEM observation. This work was partly supported by the Collaborative Research Project of Laboratory for Materials and Structures (2018-No.51), Institute of Innovative Research, Tokyo Institute of Technology, Japan.

## References

[1] M. Iwaki, K. Takahashi, K. Yoshiida, Y. Okabe, Nucl. Inst. Methods Phys. Res. B 39 (1989) 700.
[2] B.S. Elman, M. Shayegan, M.S. Dresselhaus, H. Mazurek, G. Dresselhaus, Phys. Rev. B 25 (1982) 4142.
[3] M. Kitajima, K. Aoki, M. Okada, J. Nucl. Mater. 149 (1987) 269.
[4] S. Mathew, B. Joseph, B.R. Sekhar, B.N. Dev, Nucl. Inst. Methods Phys. Res. B 266 (2008) 3241.
[5] K. Nakamura, M. Kitajima, Appl. Phys. Lett. 59 (1991) 1550.
[6] T. Kimata, S. Kato, T. Yamaki, S. Yamamoto, T. Kobayashi, T. Terai, Surf. Coat. Technol. 306 (2016) 123.
[7] T. Kimata, K. Kakitani, S. Yamamoto, I. Shimoyama, D. Matsumura, A. Iwase, W. Mao, T. Kobayashi, T. Yamaki, T. Terai, ChemRxiv (2017), https://doi.org/10.26434/chemrxiv.5554159.v1.
[8] A.C. Ferrari, Solid State Comm. 143 (2007) 47.
[9] L.G. Cançado, A. Jorio, E.H. Martins Ferreira, F. Stavale, C.A. Achete, R.B. Capaz, M.V.O. Moutinho, A. Lombardo, T.S. Kulmala, A.C. Ferrari, Nano Lett. 11 (2011) 3190.
[10] K. Ishioka, M. Hase, M. Kitajima, K. Ushida, Appl. Phys. Lett. 78 (2001) 3965.
[11] F. Gao, F. Zhou, Y. Yao, Y. Zhang, L. Du, D. Geng, P. Wang, J. Electroanal. Chem. 803 (2017) 165.
[12] H. Uehara, Y. Uemura, T. Ogawa, K. Kono, R. Ueno, Y. Niwa, H. Nitani, H. Abe, S. Takakusagi, M. Nomura, Y. Iwasawa, K. Asakura, Phys. Chem. Chem. Phys. 16 (2014) 13748.
[13] M.Y. Smirnov, A.V. Kalinkin, E.I. Vovk, P.A. Simonov, E.Y. Gerasimov, A.M. Sorokin, V.I. Bukhtiyarov, Appl. Surf. Sci. 428 (2018) 972.
[14] Y. Zhou, R. Pasquarelli, T. Holme, J. Berry, D. Ginley, R. O'Hayre, J. Mater. Chem. 19 (2009) 7830.
[15] K. Kakitani, T. Kimata, T. Yamaki, S. Yamamoto, T. Taguchi, T. Kobayashi, W. Mao, T. Terai, Surf. Coat. Technol. 355 (2018) 259.
[16] J.F. Ziegler, J.P. Biersack, U. Littmack, The Stopping Range of Ions in Solids, Pergamon Press, NewYork, 1985.
[17] Y.Y. Wang, Z.H. Ni, Z.X. Shen, H.M. Wang, Y.H. Wu, Appl. Phys. Lett. 93 (2008) 043121.
[18] K. Nakamura, M. Fujitsuka, M. Kitajima, Phys. Rev. B 41 (1990) 12260.
[19] F. Tuinstra, J.L. Koenig, J. Chem. Phys. 53 (1970) 1126.
[20] D.S. Knight, W.B. White, J. Mater. Res. 4 (1989) 385.
[21] K. Nakamura, M. Fujitsuka, M. Kitajima, Chem. Phys. Lett. 172 (1990) 205.
[22] A.C. Ferrari, J. Robertson, Phys. Rev. B 61 (2000) 14095.
[23] A.C. Ferrari, S.E. Rodil, J. Robertson, Phys. Rev. B 67 (2003) 155306.
[24] K. Bogdanov, A. Fedorov, V. Osipov, T. Enoki, K. Takai, T. Hayashi, V. Ermakov, S. Moshkalev, A. Baranov, Carbon 73 (2014) 78.
[25] G.M. Bhalerao, M.K. Singh, A.K. Sinha, H. Ghosh, Phys. Rev. B 86 (2012) 125419.
[26] K. Nakamura, M. Kitajima, Phys. Rev. B 45 (1992) 78.
[27] K.G. Nakamura, M. Kitajima, Surf. Sci. 283 (1993) 255.